

# **High Resolution Sequence Stratigraphy Correlation and Sedimentary Model of Turbidites: A Case on the 1<sup>st</sup> Member of the Kqn Formation in the Dabusu Area, South Songliao Basin\***

**Ning Zhao<sup>1</sup>, Lunkun Wuan<sup>2</sup>, Fengjun Mao<sup>2</sup>, Jiangqin Huang<sup>3</sup>, and Zhi Li<sup>2</sup>**

Search and Discovery Article #10698 (2015)\*\*

Posted January 12, 2015

\*Adapted from extended abstract prepared for a poster presentation at AAPG 42<sup>nd</sup> Eastern Section Meeting, London, Ontario, Canada, September 27-30, 2014

\*\*AAPG © 2014 Serial rights given by author. For all other rights contact author directly.

<sup>1</sup>Research Institute of Petroleum Exploration and Development, PetroChina, Beijing 100083, China ([williams8021@petrochina.com.cn](mailto:williams8021@petrochina.com.cn))

<sup>2</sup>Research Institute of Petroleum Exploration and Development, PetroChina, Beijing 100083, China

<sup>3</sup>CECEP L&T Environmental Technology, Beijing 100085, China

## **Abstract**

Based on high resolution sequence stratigraphy and sedimentology, combined with the analysis of cores, logging and seismic data, the high resolution sequence stratigraphy framework and sedimentary characteristics of turbidites in the 1<sup>st</sup> member of the Qingshankou Formation in the Dabusu area of the west slope, Southern Songliao Basin, were analyzed. According to turbidites formation and multi-grades collapses, three kinds of turbidite microfacies are identified: (1) slumps (connected with or disconnected with source), (2) turbidite channels (close to or distant from source), and (3) turbidite sand sheets (usually far away from source). Slumps usually occur in the falling periods of base level cycle (BLC), which is close to the sequence boundary (SB). Slumps are thick, superimposed, or interlaid with turbidite channels vertically and usually become thicker upwards. Turbidite channels occur in both the rising and falling periods of the BLC. In the rising periods of BLC, turbidite channels are usually thick, showing “boxing” shape on the GR log, which usually is located close to the SB and becomes thinner upwards, acting as trunks for turbidite channels. However, in the falling periods of the BLC, turbidite channels are usually thin, showing “finger” shape on the GR log, which usually occurs near the maximum flooding surface and becomes thicker upwards, acting as flanks for turbidite channels. Most of the turbidite sand sheets occur in the deep water area and near the maximum flooding surface. They are thin and superimposed with lacustrine shale or turbidite channel flanks vertically.

Considering turbidite formation (i.e. distant gentle slope, distant steep slope, or nearby steep slope), source type (i.e. point, multi-points, or linear source) and grain size (i.e. gravel rich, sand rich, or shale rich), 27 kinds of turbidites are identified. Furthermore, turbidites located in the Dabusu area are distant gentle slope, multi-points source, and shale-sand rich one.

## Introduction

Nowadays, petroleum exploration goes from relatively continental deposits and transient delta deposits to deep water deposits. The fine sediments are deposited in the deep water area, and favorable traps can be formed if there are enough sand reservoirs developed. The deep water sands are important reservoirs in lithologic petroleum exploration. More and more scholars were concerned about deep water deposits, like a series of articles about turbidite genesis published by Shanmugam between the years 2000 and 2006 (Shanmugam, 2000(a); Shanmugam, 2002(b); Shanmugam, 2003(a); Shanmugam, 2004; Shanmugam, 2006(a)), and the sequence stratigraphy published by Mulder between the years 2001 and 2003 (Mulder and Alexander, 2001; Mulder et al., 2001; Mulder et al., 2002; Mulder et al., 2003), and Walker (1978), Shanmugam and Moiola (1988), Reading and Richards (1995), and Reading and Collinson (1996) did some research on turbidite models.

In China, most of the turbidites are thick and coarse grain within sandy debris flow deposits, like the Shahejie Formation in the Dongying depression (Liu, 2008) and the Yanchang Formation in the Ordos Basin (Zhao et al., 2008). The turbidites are considered to be various fan models. However, the thin layer and fine grain turbidites are neglected. The turbidites all over the world (Table 1), including two oilfields found in California, and two discovered in the North Sea and one in Brazil, can have huge reserves, more than some conventional oilfield production. For example, the oil production of the turbidites in the 1<sup>st</sup> Member of the Qingshankou (QSK) Formation in the Dabusu Area, South Songliao Basin, exceeded 600 barrels per day from a 10 m thickness reservoir. Therefore, turbidites can be one of the favorable reservoirs in oil and gas exploration.

For the sequence stratigraphy study of turbidite deposits, there are many challenges, such as whether the sequence stratigraphy theory, which is based on the passive continental margin can be used in the deep water deposits or not; whether the sequence stratigraphy correlation is based on lithology surface or physical surface, like mutation or denudation, overlap or lithological surface; how to deal with overlaid sands correlation; and so on (Figure 1).

## Regional Setting

Songliao Basin went through three tectonic movement periods, the early rifting period from the late Paleozoic to the late Jurassic, the middle depression period from the early Cretaceous to the late Cretaceous, and the late uplift folding period from the late Cretaceous to the Neogene. The Cretaceous is the major depositional period in the geological evolution of the Songliao Basin, from the lower Ksh, Kyc, Kd, Kq, Kqn, Ky, Kn formations to the upper Ks, and Km formations. From the Kq to Ky formations, the Songliao Basin goes through the fault depression period to the depression period, as tectonic movements tend to be less and little faults are growing during the period. Meanwhile, the basin is in stable sinking and the lake area is growing wider and wider, sands are going into more deep areas, and overlapping the above underlying layers (Yang et al., 2005; Cai et al., 1999; Hou et al., 1999). The Kqn Formation is about 400-450 m thick, and the Kqn<sup>1</sup> Member is just 50-60 m thick. In high resolution theory, the Kqn<sup>1</sup> Member in the lower part of the long term base level cycles (BLC) in geological evolution time, including one integrated middle term BLC, can be further divided into two short term BLCs (Figure 2).

Dabusu area is about 1400 km<sup>2</sup>, located between the west slope and the central depression belt of the southern Songliao Basin. It has four river systems: Baicheng River 77 km in the northwest, Tongyu River 45 km in the west, Baokang River 79 km in the southwest, and Changling

River 58 km in the south (Figure 2). Sandy deposits from the Tongyu and Baokang rivers in the southwest are the major sources in the area, covering more than 10000 km<sup>2</sup> during the early Cretaceous Period (Yang et al., 2005; Bo, 2003), compared with the Baicheng River in the northwest covering nearly 2400 km<sup>2</sup>. Although the Changling River in the south is nearly 4200 km<sup>2</sup> (Bo, 2003), it is blocked by the central depression belt and little debris is deposited. Therefore, most of the deposits in the Dabusu area come from the west slope and southwest uplifted zones, undergoing long distance transportation.

### **High Resolution Sequence Stratigraphy Framework**

In the theory of high resolution sequence stratigraphy (HRSS), (1) base level is a potentiometric surface, and (2) high Accommodation/Sedimentary supply (A/S). Sedimentary facies preservation is good, vertical gradation is clear, and sands are isolated distributed vertically. However in low A/S, sedimentary facies preservation is bad, vertical gradation is unclear, and sands are superposed vertically. According to the variation of accommodation and sediment supply, base level shows a dynamic balance, and depositional volume is changing according to different depositional environment. Therefore, a new correlation standard is created in the sequence stratigraphy correlation, not restricted to unconformities, and rising and falling periods of BLC can be identified according to the A/S change. Moreover, the HRSS correlation is adaptable to multi-periods deposits, especially overlaid sands correlation.

For accurate HRSS correlation, three steps can be followed: (1) Choosing a stable, large distribution, and easy tracing marker. According to well logs and seismic data in this area, 20 m thick shales in the Kqn<sup>2</sup> Member, usually 45-50 m above the top of Kqn<sup>1</sup> member, is selected as the marker in the area (Figure 3). (2) Identifying the rising or falling periods of multi-grades BLCs, as Q1-1 and Q1-2 secondary cycles in the Kqn<sup>1</sup> member (Figure 3). (3) Considering sediment distribution both lateral and planar in HRSS correlation. Compared with well sections both vertical and parallel to the source supply direction (SSD), strata trend/dip direction and bed thickness are different. Vertical to the SSD, the strata is always uneven, fluctuated, and bed thickness is frequently changing. Parallel to the SSD, the strata inclines toward the southeast (Figure 4), and bed thickness is rarely changed (Figure 4).

### **Sedimentary Characteristics of Turbidites**

#### **Turbidite Flume Experiments**

In order to make clear about mechanisms of turbidites formation, turbidite flume experiments were conducted by China University of Petroleum (Beijing) in 2007. There are three kinds of mechanisms in turbidites formation: earthquake, compaction and subsidence, and wave flapping.

#### **Earthquake**

Earthquake, caused by tectonic movement, is very common in nature. In the experiment, sands can be divided into the liquefied and the collapsed part. When the focus (earthquake center) vibrates, sands near the focus liquefy and discharge to the nearby area (Figure 5B). Meanwhile, sands away from the focus collapse and slide down through faulted steps (Figure 5C and Figure 5D), and go into the more distant

and deep area, where a large amount of multi-grades slumping turbidites can be formed (Figure 5B). The primary slumps are usually near the slope toe, which have a ligulate shape generally (Figure 6B). The secondary slumps or lower grade slumps locate in the further deep area, which usually have an elliptical shape (Figure 6C).

### **Compaction and Subsidence**

When lower shales can not sustain upper sands gravity, with more and more sands overlaying continuously, lower shales get thinner and thinner, and slumping will happen eventually (Figure 7B). Upper sands liquefy and go through narrow channels (Figure 7C) into the deep water area. With delta front sands progradation and retrogradation, multi-periods of turbidites can be formed and superimposed vertically (Figure 7D).

### **Wave Flapping**

When wave are continually flapping on delta sands on the slope break, sands would be liquefied (Figure 8B), and slide down to the slope toes (Figure 8A). Most primary slumps are formed under the maximum wave base level (Figure 8C) in the local area, and secondary slumps are not well developed for the continually wave flapping onto the slope break.

## **Sedimentary Facies of Turbidites**

According to the turbidite flume experiments above, core observation, well logs, and seismic data, three kinds of sedimentary microfacies are identified: slumps, turbidite channels, and turbidite sand sheets.

### **Slumps**

Slumps are formed by continuous or uncontinuous blocks sliding from the upper slope break to the lower slope toe, which is caused by some external trigger (e.g. earthquake) or sands gravity (e.g. compaction and subsidence). They are always a fan, crumb or irregular shape, including two types (Figure 9B). One is connected with the source supply, which usually has a large distribution, and a fan, tongue, or stripe shape. It has a relatively high-sand content, with coarse grain size; the other is separated from the source supply (Moscardelli and Wood, 2008), which has a narrow distribution, and a stripe or belt shape. It has a relative low sand content, with fine grain size. The latter is the major type developed in the area.

Slump characteristics are as follows: (1) Most of them are blue gray, gray or green color, finestones or slitstones, with dark and thin shale or carbonate layers. (2) Typical beddings included convolute or deformed beddings, or irregular high-angle dip beddings (Wang, 2005). Broken pile-up deposits, stripped sandy blocks or sandy to shaly bricks and erosion bottoms are very common in slumps. (3) They have an anticycle characteristics in well logs and infundibulate shapes on GR, SP, and AC logs and bell shape on the R25 log (a kind of resistivity, Figure 10A), indicating an inverse cyclicity. (4) Weak amplitude, uncontinuous and worm shape in seismic sections. (5) Great variation in the thickness of sand layers, between 2.4 and 9 m, most of them are 4-5 m thick.

## **Turbidite Channels**

Turbidite channels are stripped piled-up sands, moving from the slope break through one main channel (strong flow power) or several channels (weak flow power) into the deep water area of a lake or sea basin. They are caused by some external trigger or sand's gravity and usually have a trough or stripped shape in seismic sections. According to log characteristics, turbidite channels can be divided into two types. One is the channel trunk, with a boxy shape on GR log, usually developed in the rising periods of BLC. The other is the channel flank, with a finger shape on GR log, usually developed in the falling periods of BLC.

Turbidite channel characteristics are as followed: (1) Most of them are finestones, slitstone or shaly slit stone. (2) Splitted pieces, pillow structures, and liquefaction structures are very common in them. (3) Block beddings, deformed beddings, and wave beddings are well developed in them (Figure 10A). (4) Grain size analyses (i.e. the cumulative probability of grain size and C-M figure) show two compositions, including suspending and jumping particles (Figure 10B and Figure 10C). (5) A belly or blocky shape on GR, SP, and AC logs and a funnel or boxy shape on R25 log. In log characteristics, they show a quick changing at the bottom, a gradual changing at the top, and usually go thinner upwards, indicating a positive cyclicity. (6) Weak amplitude, uncontinuous and a worm or buninoid shape in seismic sections. (7) Various changes in sand layers thickness, most of them are 2-5 m thick, and multi-periods of overlaid sand layers are usually 2.3-7 m thick.

## **Turbidite Sand Sheets**

Turbidite sand sheets are a tongue, sheet, or elliptical shape with fine sands and shale mixture caused by sand liquefaction, compression and depression, or wave flapping. They usually occur on the edge of slumps or turbidite channels with fine grain, thin layer, and have a large distribution. Compared with beach sand in the offshore or shallow lake environment, they have a higher shale content and a worse sand continuity.

Turbidite sand sheet characteristics are as followed: (1) Most of them are siltstones, argillaceous siltstones, or mudstones. (2) Deformed beddings, wave beddings, stir-up structures are well developed in them. (3) Obviously a thin figure shape on GR, SP, AC, and R25 logs (Figure 10). They are usually multi-period, overlaid vertically, and have no cyclicity in regular. (4) It is hard to identify in any seismic section because of their thin thickness. (5) Sand layers are thin and most of them less than 1 m and multi-period overlaid sand layers are usually 1.5-4.3 m thick.

## **Turbidites Distribution and Sedimentary Models**

### **Vertical Distribution of Turbidites**

Using well log correlation and seismic sections, multi-grades slope breaks can be identified, including the primary and the secondary slope breaks. The former is between delta front sands and turbidite slumps, and controls turbidites formation and sedimentary microfacies types (as the slope break between Hua28 and Hua26, between Hua19 and Hua7 in Figure 11). Turbidites usually occur in a shallow lake area with a steep slope, having a relatively large scale distribution. The latter is inside the turbidite's depositional areas, controlled by the local

paleotopography, and has an influence on turbidite sand distribution and thickness (as the slope break between Hei47 and Hei59 in [Figure 11](#)). Turbidites usually occur in a deep lake area with a gentle slope, having a relatively small scale distribution. Compared with two sections of parallel to and vertical to the SSD, the continuity of turbidite sand is totally different and microfacies of these sands are developed in different areas as the A/S change.

From northwest to southeast direction (parallel to the SSD in [Figure 11](#) the upper one), a gentle slope slightly inclines to the south. The source supply comes mainly from delta front deposits in the northwestern Dabusu area. Most of them are overlaid subaqueous distributary channels (usually 3-4 m thick) and sand sheets (usually 2-3 m thick) with little mouth bars which show good sand continuity. However, from southwest to northeast direction (vertical to the SSD in [Figure 11](#) the lower one), undulate slopes are developed. The source supply comes from three directions, i.e. from northwest to southeast direction (as in well Hua 3), from west to east direction (as in well Hua 8), and from southwest to northeast direction (as in well Hua 28). Most of the sands are subaqueous distributary channels and mouth bars (4-6 m thick) with some sand sheets (1-2 m thick) which show poor sand continuity.

In the rising periods of BLC, overlaid subaqueous distributary channels are well developed and sands flow through slope break into the deep water area. Turbidite channels are well developed in these periods, usually 3-5 m thick ([Figure 11](#)). Some of them are very thick (as well Hua26 in [Figure 11](#)), more than 10 m, which have a boxy shape on the GR log. They usually form the trunk or main part of turbidite channels. Others are thin (as well Hei59 in [Figure 11](#)), usually 2-3 m thick, which have a finger shape on the GR log. They often form as the flank or edge of turbidite channels. Therefore, in this way, turbidites flow direction can be analyzed.

In the fallings period of BLC, mouth bars and sand sheets are well developed and slumps are usually caused by mouth bar sands sliding through the slope break. Slumps are usually bellow the primary slope break, usually near the slope toe (as well Hua7 in [Figure 11](#)). Turbidite sand sheets are always near the maximum flooding surfaces, which are relatively far away from the primary slope break in the deep area and usually 1-2 m thick. Turbidite sand sheets are caused by multi-periods turbidite channels overlaying vertically and sliding into the deeper area where sands are unloaded with the decreasing of flow power. Turbidite sand sheets are muti-periods overlaid vertically and usually have a sheet shape distribution.

As the A/S is decreasing upwards, slumps and tubidite channels are more and more developed near the slope toes. The sand continuity is relatively poor as the A/S is increasing upwards. Turbidite sand sheets are more and more developed away from the slope toes and sand continuity is good.

### **Planar Distribution of Turbidites**

In order to describe sedimentary facies precisely, the slope break position and the slope gradient and length should be considered. Condisidering the short period of the Kqn<sup>1</sup> Member (about 11.5 Ma) and a stable depression tectonic backgroud of the Songliao Basin (about 0.877 million km<sup>2</sup> lake area during the Kqn<sup>1</sup> Member), the slope break position can be reagarded as relatively stable or fixed. With sedimentary microfacies analysis in 57 wells, seismic attribute extraction and statistics of turbidite sands thickness in the rising and falling periods of BLC in the Kqn<sup>1</sup> Member of the Dabusu area are conducted.



In seismic attribution maps, thick lake shales show dark color and the relatively thin delta front or turbidite sands show bright color as the thick shales intercalated with relative thin sands. Compared with other kinds of seismic attribution extractions, RMS is the most accurate data to indicate turbidite sands (the central area in [Figure 12A-C](#)), delta front (the west area in [Figure 12A-C](#)) sands distribution, and the exact slope break location in the  $Kqn^1$  member. It is the best method to predict thin-layer sand distribution for different seismic amplitude responses in shales and sands.

According to bed thickness, sand thickness, and sand to bed ratio distribution calculated by 57 wells ([Figure 12D-F](#)) two SSDs are represented. Among them, the major SSD comes from the northwest to southeast direction and the secondary SSD comes from the southwest to northeast direction. Most of the turbidites occur in the central and southeastern area. With the analysis of turbidite microfaeces of all wells, turbidite sand distribution area and thickness are controlled by the SSD ([Table 2](#)). When the source supply is sufficient, turbidites distribute in a large area with good sand continuity ([Figure 13A](#)). When the source supply is insufficient, turbidites distribute in a relatively small area with poor sand continuity ([Figure 13D](#)). From the  $Kqn^{1-2}$  to the  $Kqn^{1-1}$  epoch, most delta front sands coming from the southwestern area turn into the northwestern area as the A/S is increasing upwards. The long axis of the turbidite sands also follows the same alteration of direction ([Figure 13C](#)) and the depositional center of turbidites moves from the center to the southern area. In the rising periods of BLC, the accommodation space goes faster than the sediments supply. Sands above the slope break slide into the deep area and turbidite channels are grown. With the water buoyancy and lubrication, sands move forward and go into the more deep area ([Figure 13B](#)).

Lots of turbidite channels are superposed together in the rising and falling periods of BLC and turbidite sand sheets are at the edge of the turbidite channels. In the falling periods of BLC, the accommodation space grows slower than the sediments supply. Sands move forwards and go through the slope break into the deep area. Coarse grain slumps are grown close to the slope break with lots of fine grain turbidite sand sheets in the more deep area. Considering good sorting, thickness, and distribution area the rising periods of BLC are more favorable for turbidite reservoirs in petroleum exploration than the falling periods, especially the rising period of the  $Kqn^{1-1}$  Member ([Figure 13B](#)).

## **Turbidite Depositional Models**

Shanmugam and Moiola, 1988 suggested two submarine fan models like attached and detached lobes. Reading and Richards, 1995 concluded 12 kinds of turbidite models according to source type and grain size, but they did not consider the paleotopography like steep slope or gentle slope and mechanisms like earthquake, subsidence, or wave flapping. According to source type (point source, multi-point source, and linear source), bed structure (distant gentle slope, distant steep slope, and nearby steep slope), and grain size (gravel rich, sand rich, and shale rich), 3 classes and 27 types of turbidite models are concluded:

1. In the distant gentle slope of turbidites, slumps are not well developed ([Figure 14](#)) for the gentle slope.
2. As the grain size goes smaller, turbidite channels are less developed for the weaker flow power.
3. From point source to linear source, turbidite channels are more and more developed for sufficient source supply and usually overlaid vertically.

Former scholars studied turbidite models of this area and most of them considered it to be a fan model, like a slumping turbidite fan (Wang, 2008) or a deep lake fan (Wang, 2005). However, (1) The tectonic background is in a stable subsiding with no regional unconformity in that period. (2) The paleotopography of this area is a gentle slope as a whole, higher in the west and lower in the east. (3) The source supply is about 40-80 km away from the area. (4) Most of the sands are fine grain, usual finestones, slitstones, shale slitstones, and mudstones. (5) Turbidite distribution is in a clear zonation with a discontinuous, blocky shape in plane view (Figure 14). (6) The average water depth in the area during the Kqn<sup>1</sup> Member is shallow, about 30-35 m deep (Zhang and Ren, 2003). Also, considering the above sedimentary characteristics, turbidites in this area are the distant steep slope, multi-point source, sand rich type.

### **Conclusions**

Take the turbidites of the Kqn<sup>1</sup> Member of the west slope in the Dabusu area, South Songliao Basin as an example, high resolution sequence stratigraphy framework is established. Challenges on the analysis of thin-layer sand correlation in turbidites can be solved effectively by applying the theory of HRSS. The A/S change can be used in the explanation on both sequence stratigraphy correlation and sedimentary faces analysis. According to bed structure, source type, and grain size, 27 types of turbidite models can be concluded. Turbidites developed in the Kqn<sup>1</sup> Member of the Dabusu area are the distant steep slope, multi-point source, sand rich type.

Turbidites can be classified into three kinds of deposits:

1. Slumps can be divided into two types, connecting with or separating from the source supply. They usually have a narrow distribution, a stripe or belt shape, and have a large thickness. Most of them occur in the falling periods of BLC, superposed or interlaid with turbidite channels vertically.
2. Turbidite channels are usually a trough or stripped shape with fine grain and thin layers. They can be divided into two types. One is the turbidite channel trunk with a box shape on the GR, which is usually in the rising periods of BLC becoming thinner upwards. The other is the turbidite channel flank with a finger shape on the GR, which is usually in the falling periods of BLC becoming thicker upwards.
3. Turbidite sand sheets are a tongue, sheet, or elliptical shape with fine grain, thin layer, and a large area distribution. They usually occur near the maximum flooding surface, superposed with lacustrine shales, channel flanks, or slumps vertically.

### **Acknowledgements**

This article is based on my PhD dissertation in China University of Geosciences (Beijing) and some ideals on turbidite models. I would thank my teacher professor Deng Hongwen, vise teacher senior engineer Shi Qiang for giving me great instruction, and also thank my parents and my wife Huang Jiangqin for giving me a great support to finish this paper work.

### **Selected References**

Bo, T., 2003, The implication of basin for several provenances - Take the south of Songliao Basin during Qingshankou term and Yaojia term as an example [D]: Journal of Jilin University, v. 33/4, p. 469-473.



- Cai, X., Z. Chen, and Y. Wang, 1999, Petroleum geological characteristics analysis of two river areas in Songliao Basin: Beijing, Petroleum Industry Press, p. 35-36.
- Hou, D., Q. Huang, and F. Huang, 1999, The characteristics of molecular geochemistry of marine transgression strata in Songliao Basin: *Acta Petrolei Sinica*, v. 20/2, p. 30-34.
- Li, C., 2005, Study on the forming mechanism of the slumped turbidite and the controlling sand body model of high frequency base-level cycle of Dongying delta: Beijing, China University of Geosciences, p. 26-53.
- Liu, Y., 2008, Formation mechanism of turbidite reservoirs in Sha3 member of Shahejie Formation, Dongying Depression: *PGRE*, v. 15/2, p. 16-19.
- Moscardelli, L., and L. Wood, 2008, New classification system for mass transport complexes in offshore Trinidad: *Basin Research*, v. 20, p. 73-98.
- Mulder, T., J.P.M. Syvitski, S. Migeon, J. Faugeres, and B. Savoye, 2003, Marine hyperpycnal flows: initiation, behavior and related deposits: A review: *Marine and Petroleum Geology*, v. 20, p. 861–882. doi:10.1016/j.marpetgeo.2003.01.003
- Mulder, T., S. Migeon, B. Savoye, and J. Faugeres, 2002, Inversely graded turbidite sequences in the deep Mediterranean: A record of deposits from flood-generated turbidity currents?: *Geo-Marine Letters*, v. 22, p. 112–120. doi:10.1007/s003670100071
- Mulder, T., and J. Alexander, 2001, The physical character of subaqueous sedimentary density flows and their deposits: *Sedimentology*, v. 48, p. 269–299. doi:10.1046/j.1365-3091.2001.00360.x
- Mulder, T., S. Migeon, B. Savoye, and J. Faugeres, 2001, Reply to discussion by Shanmugam on (Mulder et al., 2001, *Geo-Marine Letters*, 21, 86–93) Inversely graded turbidite sequences in the deep Mediterranean. A record of deposits from flood-generated turbidity currents?: *Geo-Marine Letters*, v. 21, p. 86–93. doi:10.1007/s00367-002-0096-8
- Mulder, T., O. Weber, P. Anschutz, F. Jorissen, and J.M. Jouanneau, 2001, A few months-old storm-generated turbidite deposited in the Capbreton Canyon (Bay of Biscay, SW France): *Geo-Marine Letters*, v. 21, p. 149–156. doi:10.1007/s003670100077
- Reading, H.G., and J.D. Collinson, 1996, Clastic coasts, *in* H.G. Reading (ed.), *Sedimentary Environments: Processes, Facies and Stratigraphy*: Oxford, Blackwell Science, 688 p., ISBN: 0632036273, p. 154–231.
- Reading, H.G, and M. Richards, 1995, Turbidite systems in deep water basin margins classified by grain size and feeder system: *AAPG Bulletin*, v. 78, p. 792-822.

- Shanmugam, G., 2006, Deep-water processes and facies Models: Implications for sandstone petroleum reservoirs: Elsevier, New York v. 5, ISBN: 978-0-444-52161-3, 476 p. doi:10.13140/2.1.3941.3449
- Shanmugam, G., 2006a, The tsunamite problem: Journal of Sedimentary Research, v. 76, p. 718-710. doi:10.2110/jsr.2006.073
- Shanmugam, G., 2004, Modern deep-water environments: implications for sandstone petroleum reservoirs: Promoting excellence in exploration for more oil and gas, Technical Session: Sedimentology and depositional modeling with special reference to deep-water basins. Khajuraho, India: Proceedings of the 2<sup>nd</sup> APG (Association of Petroleum Geologists) Conference and Exhibition, v. 14.
- Shanmugam, G., 2003, Deep-marine tidal bottom currents and their reworked sands in modern and ancient submarine canyons: Marine and Petroleum Geology, v. 20, p. 471-491. doi:10.1016/S0264-8172(03)00063-1
- Shanmugam, G., 2003a, A preliminary experimental study of turbidite fan deposits discussion: Journal of Sedimentary Research, v. 73, p. 838-841. doi:10.1306/101002730838
- Shanmugam, G., 2002, Ten turbidite myths: Earth-Science Reviews, v. 58, p. 311-341. doi:10.1016/S0012-8252(02)00065-X
- Shanmugam, G., 2002a, Discussion on (Mulder et al. 2001, Geo-Marine Letters, 21, 86-93) Inversely graded turbidite sequences in the deep Mediterranean. A record of deposits from flood-generated turbidity currents?: Geo-Marine Letters, v. 22, p. 108–111. doi:10.1007/s00367-002-0100-3
- Shanmugam, G., 2002b, Deep-water processes and turbidite facies models: a paradigm shift, *in* S.N. Swamy and P.N. Kapoor, (eds.), Stratigraphic Challenges and Paradigm Shift in Hydrocarbon Exploration with Special References to Frontier Basins, Mussoorie, India: Proceedings of the 1<sup>st</sup> APG (Association of Petroleum Geologists) Conference and Exhibition, v. 1, p. 155–162.
- Shanmugam, G., 2000, John E. Sanders and the turbidite controversy: Conference on the History of Geologic Pioneers, Troy, New York, Rensselaer Center of Applied Geology, p. 19-20. doi:10.13140/2.1.1713.1202.
- Shanmugam, G., 2000a, 50 Years of the turbidite paradigm (1950s-1990s): deep-water processes and facies models - a critical perspective: Marine and Petroleum Geology, v. 17, p. 285-342. doi:10.1016/S0264-8172(99)00011-2
- Shanmugam, G., and R.J. Moiola, 1988, Submarine fans: characteristics, models, classification, and reservoir potential: Earth Science Reviews, v. 24/6, p. 383-428. doi:10.1016/0012-8252(88)90064-5
- Walker RG., 1978, Deep-water sandstone facies and ancient submarine fans: models for exploration for stratigraphic traps: AAPG Bulletin, v. 62, p. 932-966.

Wang, H., 2008, Concept of “Turnaround Surface” and its significance to sequence stratigraphy: *Earth Science Frontiers*, v. 15/2, p. 35-42.

Wang, Y., 2005, The controlling of slope belt on sediment and lithological and stratigraphic traps in large-scale down warped lacustrine basins, a case study in the south of Songliao Basin: Beijing, China University of Petroleum.

Wang, Y., 2005, Stage reports in non-structural traps of west slope in southern Songliao Basin (internal reports in CNPC).

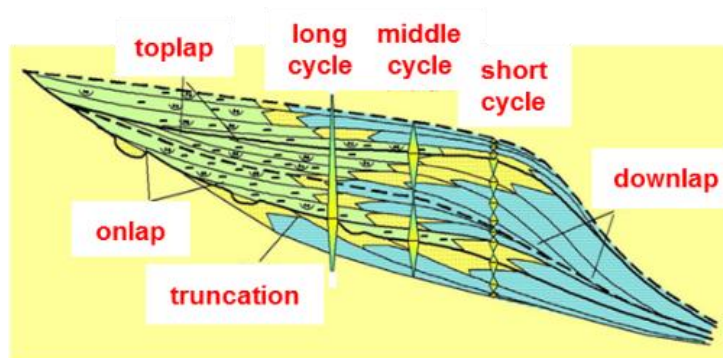
Wei, P., J. Wang, and S. Pan, 2004, Formation of the Mouth Bar and Lakeshore Bar and Their Petroleum Accumulation—An example of southern and western depositional systems in Songliao Basin: *Xinjiang Petroleum Geology*, v. 25/6, p. 592-595.

Weimer, P., and R.M. Slatt, 2004, *The Petroleum Systems of Deep-Water Settings: SEG Distinguished Instructor Short Course Notes*, 488 p.

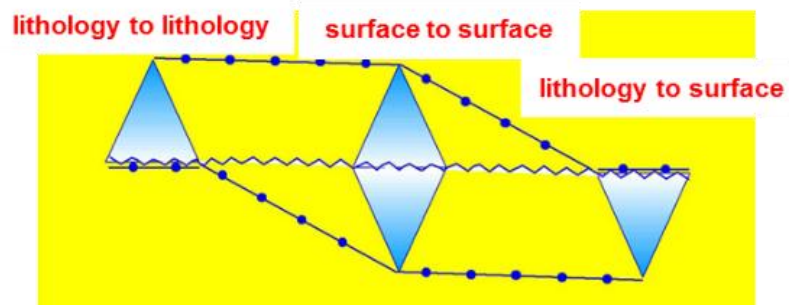
Yang, H., S. Wang, Y. Ma, 2005, Application of high resolution sequence stratigraphy to exploration of subtle reservoir in the southern Songliao Basin: *Acta Petrolei Sinica*, v. 26/3, p. 40-43.

Zhang, S., and Y. Ren, 2003, The study of base level changes of the Songliao Basin in Mesozoic: *Journal of Chang'an University (Earth Science Edition)*, v. 25/3, p. 1-5.

Zhao, J., F. Li, and X. Sehn, 2008, Sedimentary characteristics and development pattern of turbidity event of Chang 6 and Chang 7 oil reservoirs in the southern Ordos Basin: *Acta Petrolei Sinica*, v. 29/3, p. 389-394.



### Adaptability of Sequence Stratigraphy



### Correlation Standard

### Continuity of sand correlation

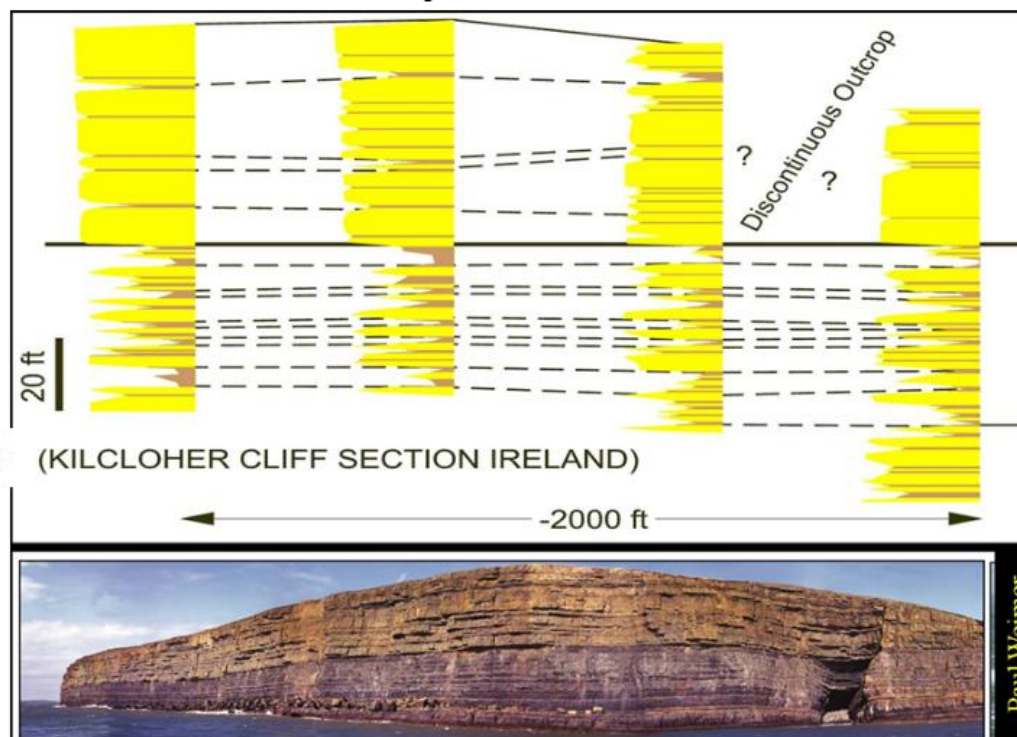


Figure 1. Challenges in sequence stratigraphy of turbidite deposits: Upper-left Figure shows the sequence stratigraphy theory raised from passive continental margin; Lower-left Figure shows the correlation standard sequence stratigraphy; Right Figure shows continuity of sand correlation by Weimer and Slatt, 2004.

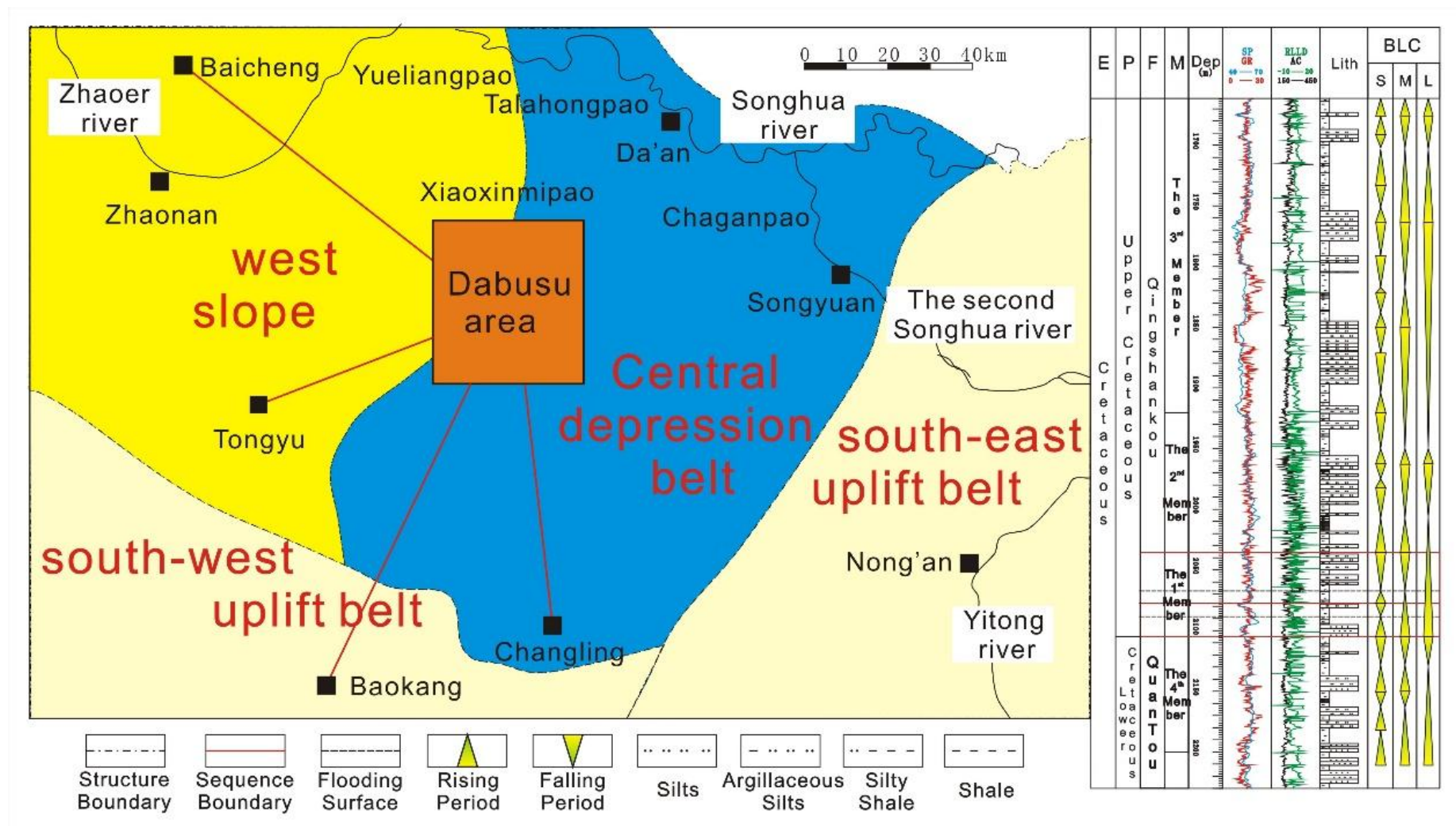


Figure 2. Geographical location and comprehensive strata histogram of the Dabusu Area, Jilin (F=Formation, M=Member, Dep=Depth, Lith=Lithology, S=short term, M=medium term, L=long term, BLC=Base Level Cycle).



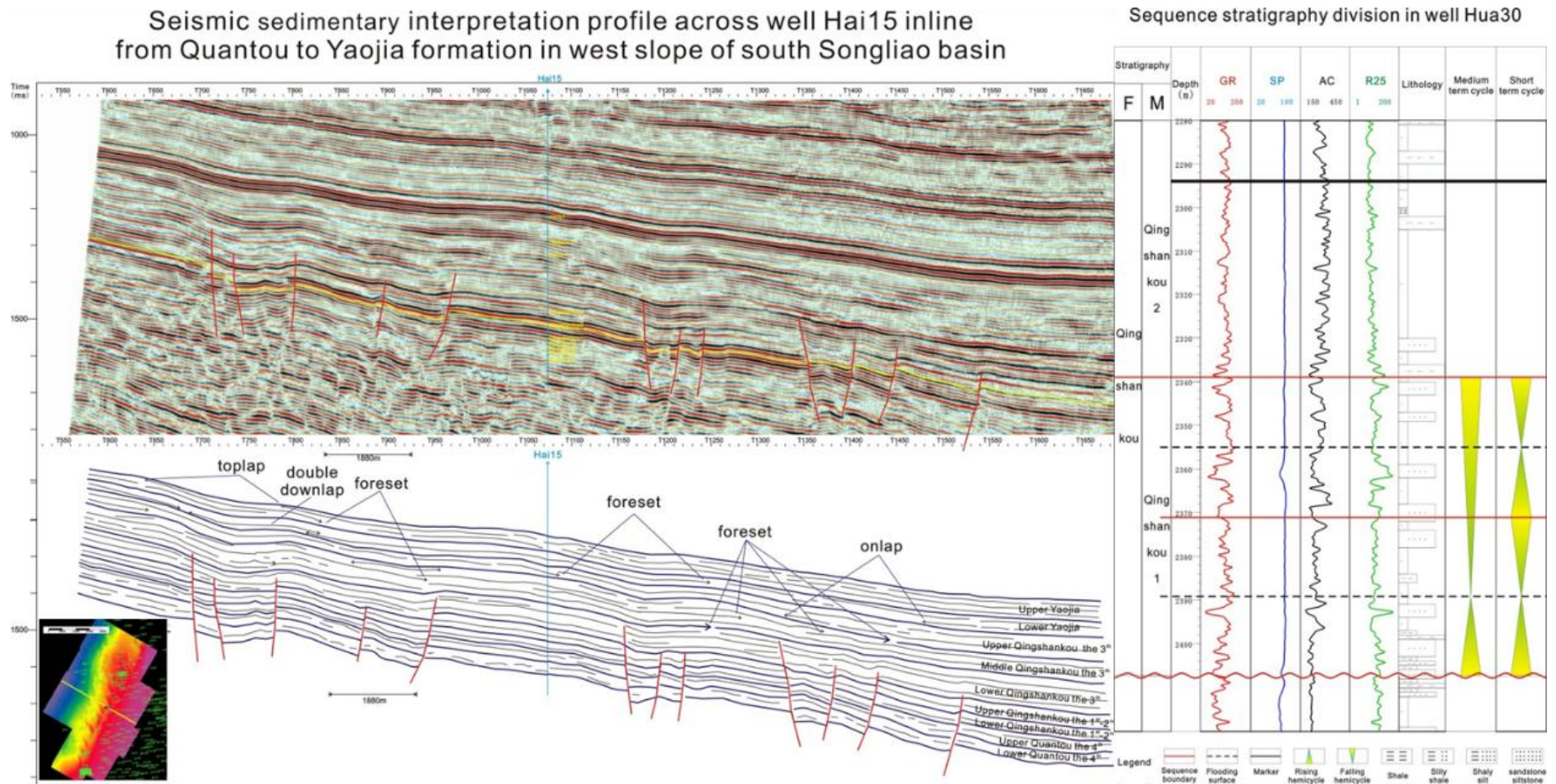


Figure 3. High resolution sequence stratigraphy framework (the left Figure is the seismic section of the inline across well Hai15 and sequence division; the right Figure is the high resolution sequence division in well Hua30).



## Sequence stratigraphy correlation of Q1 member in Dabusu area, SW Songliao basin

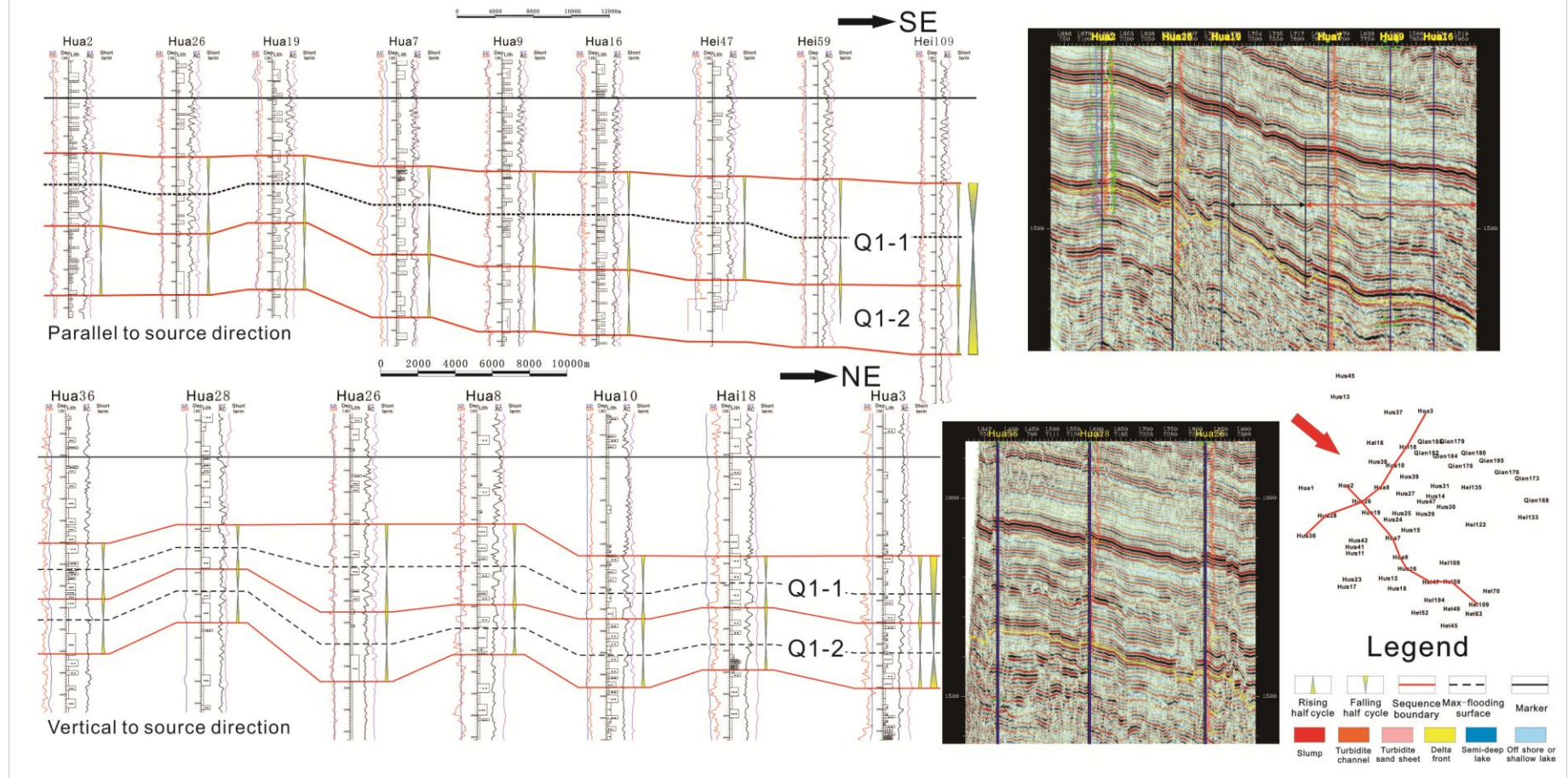


Figure 4. High resolution sequence stratigraphy correlation (The upper Figure is vertical to the SSD. The lower Figure is parallel to the SSD.).

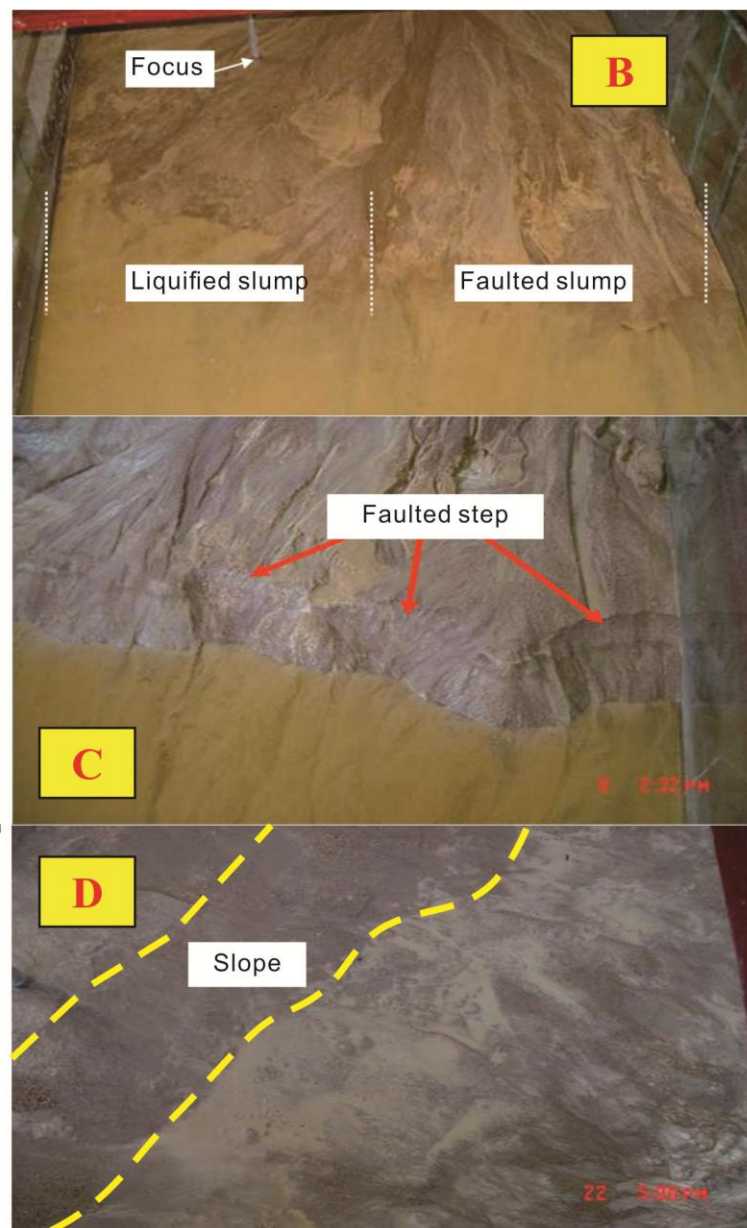
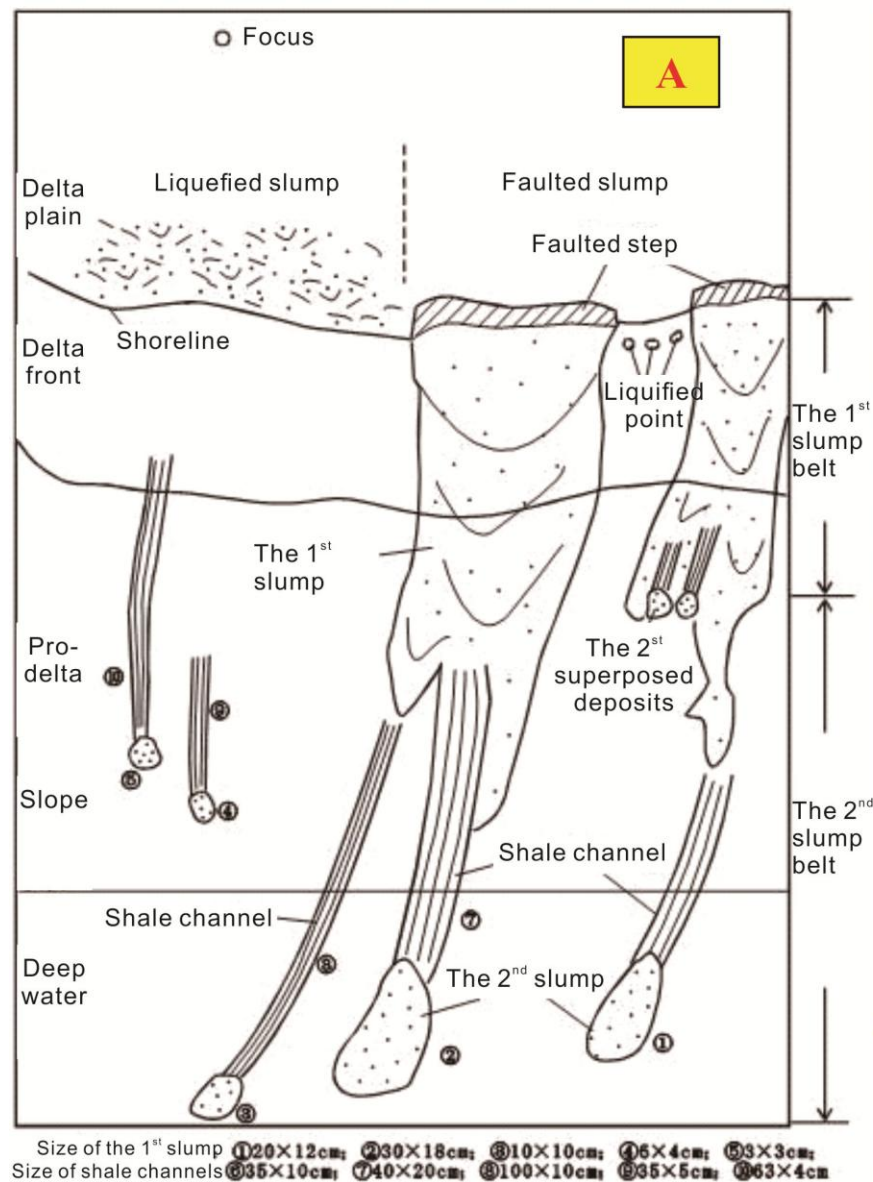


Figure 5. Flume experiments and conceptual model of earthquake formation. This experiment was done at the China University of Petroleum, Beijing. The initial slope gradient is 8°. A: Manuscript of earthquake mechanism of turbidite formation (Li, 2005). B: Liquefied and faulted slumps in different areas. C: Faulted steps in slope. D: Slope boundary in turbidite formation.



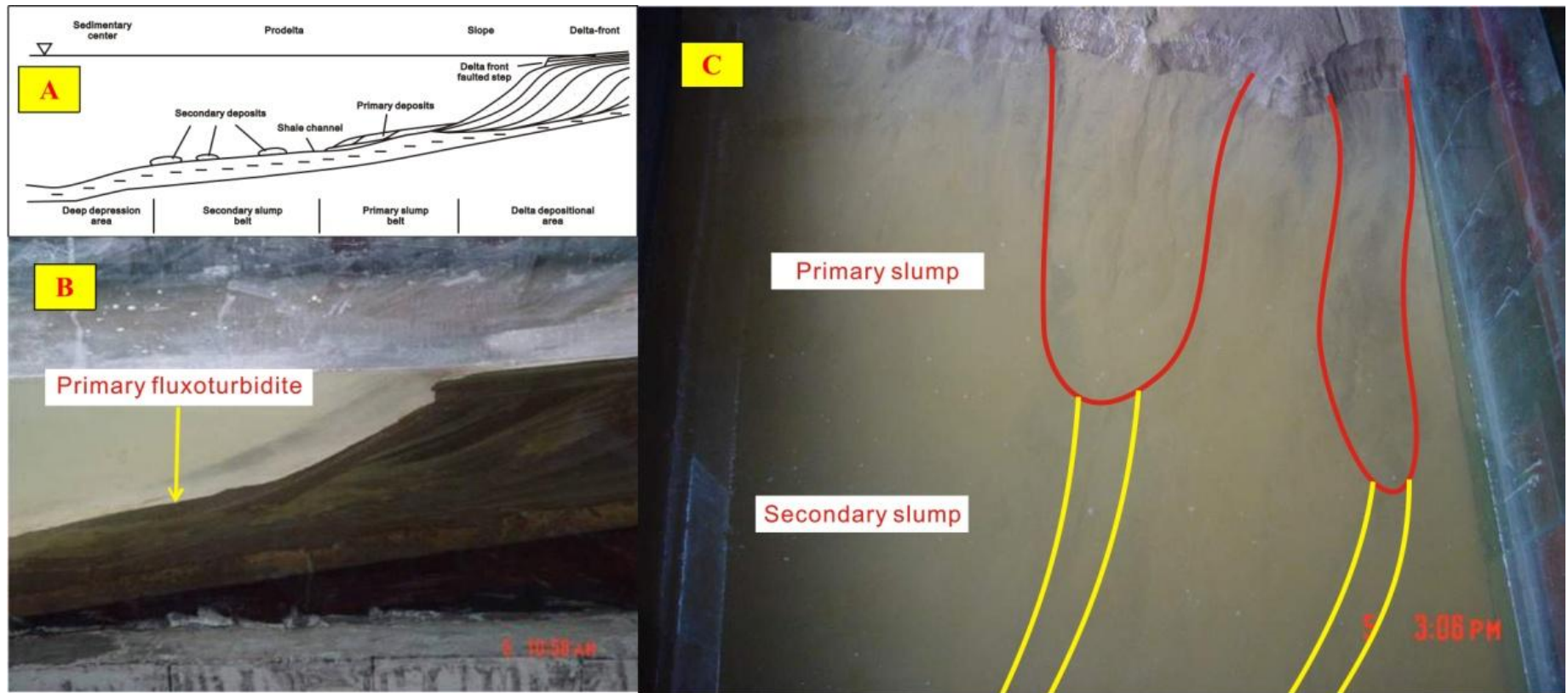


Figure 6. Flume experiments and the conceptual model of earthquake mechanism. A: Turbidite formation manuscript (Li, 2005). B: The primary fluxoturbidites in the experiment. C: The primary slumps and the secondary slumps in different periods.

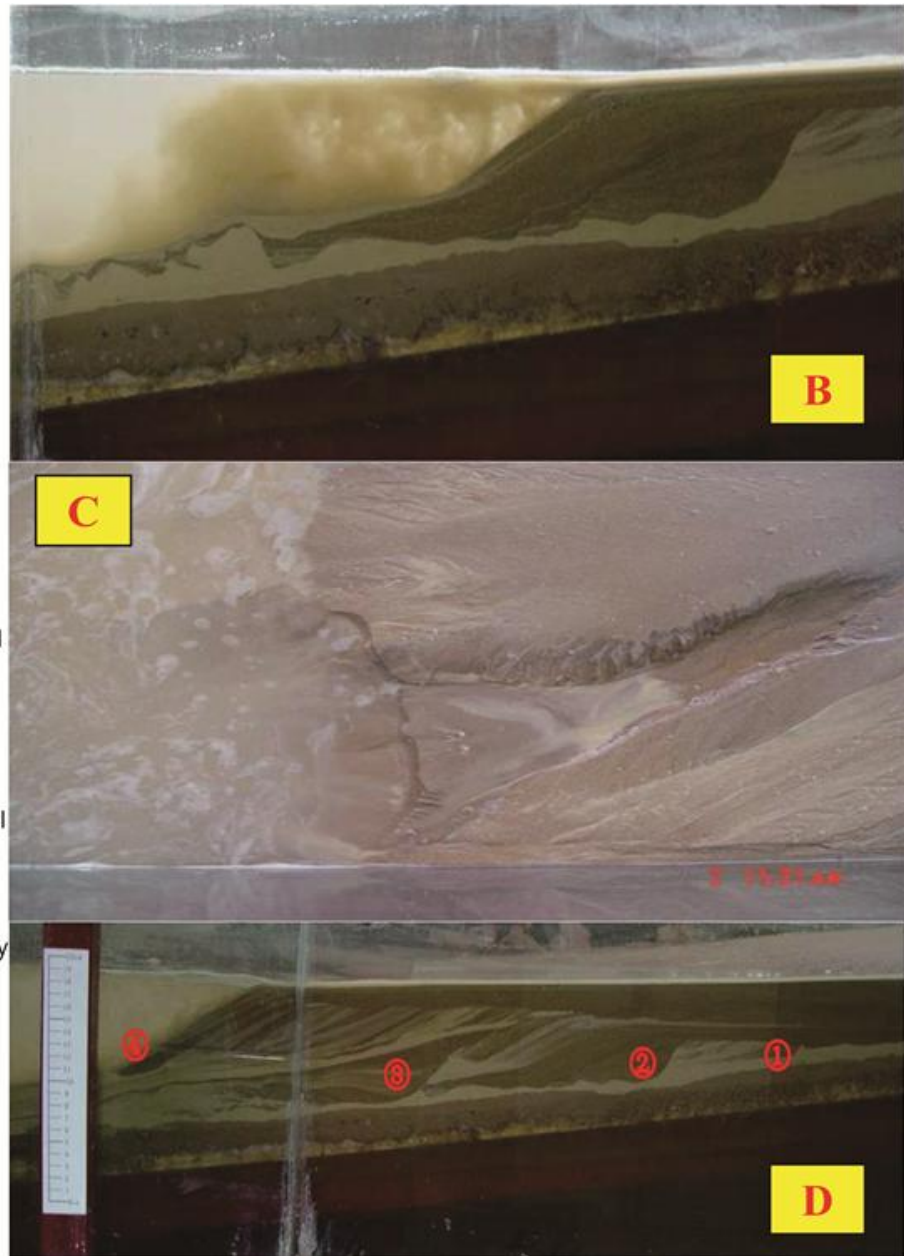
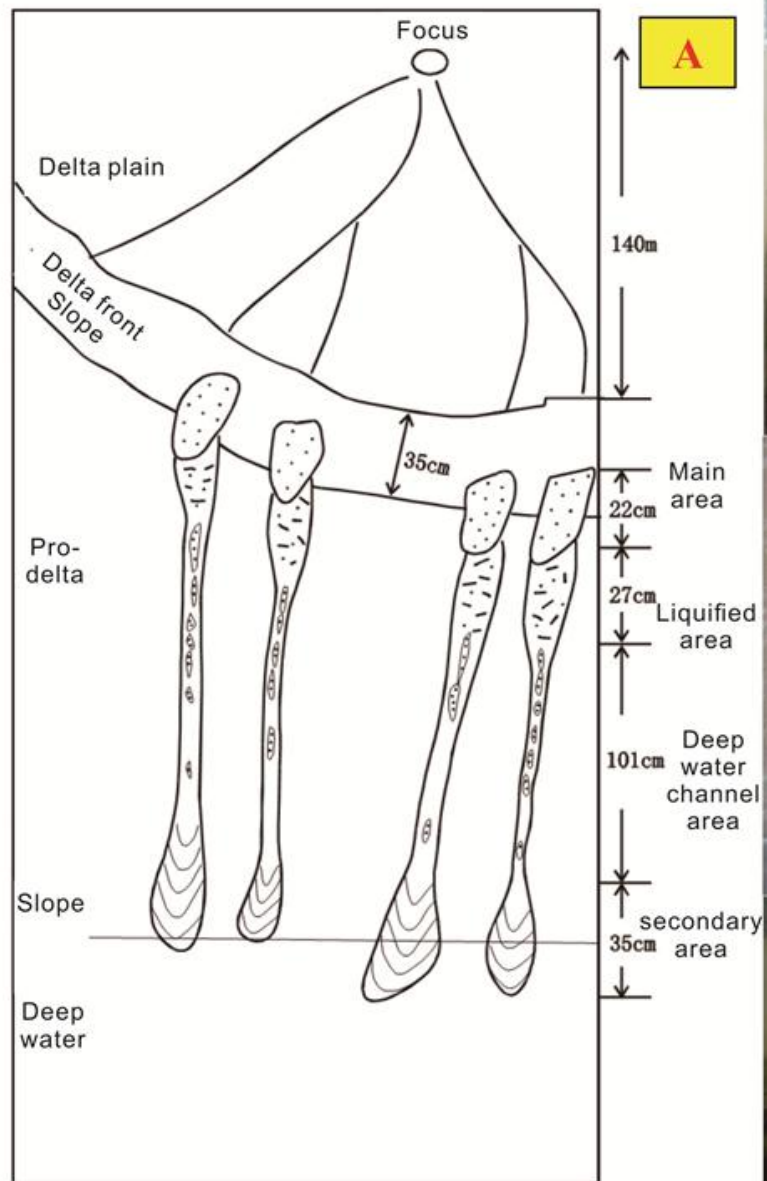


Figure 7. Flume experiments and the conceptual model of compaction and subsidence mechanism. A: Turbidite formation manuscript (Li, 2005). B: Lower shales are thinner and thinner. C: The slump happens and sands liquefy. D: Multi-periods of turbidites are overlaid vertically.

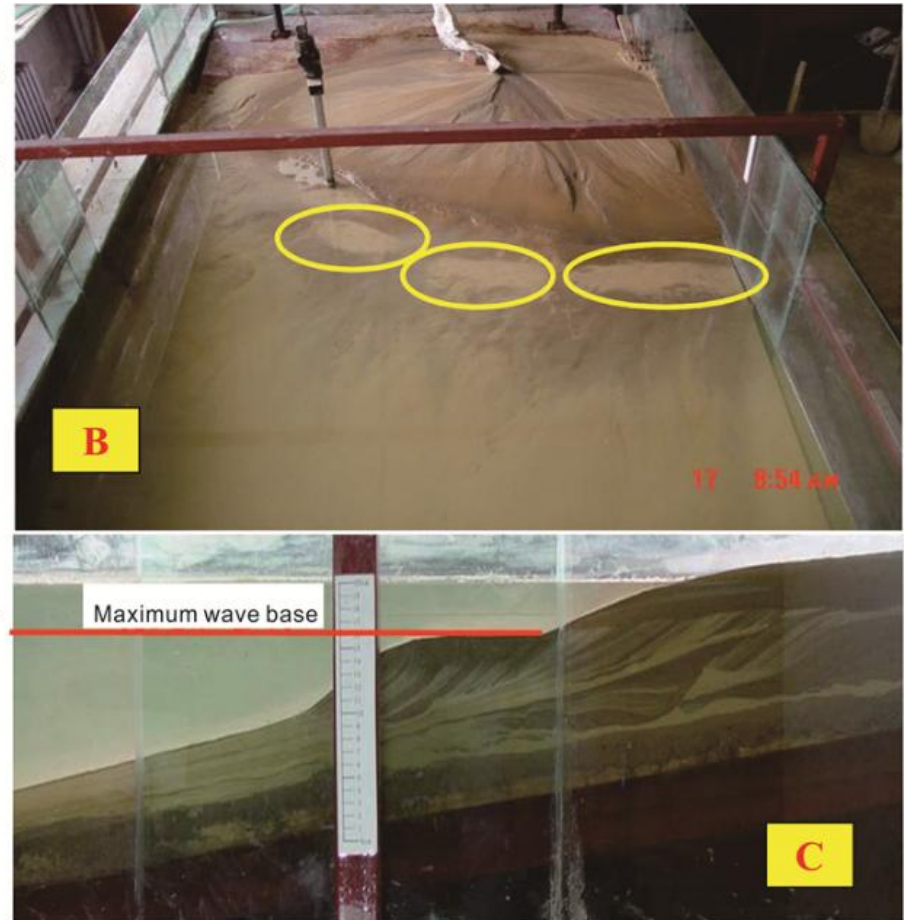
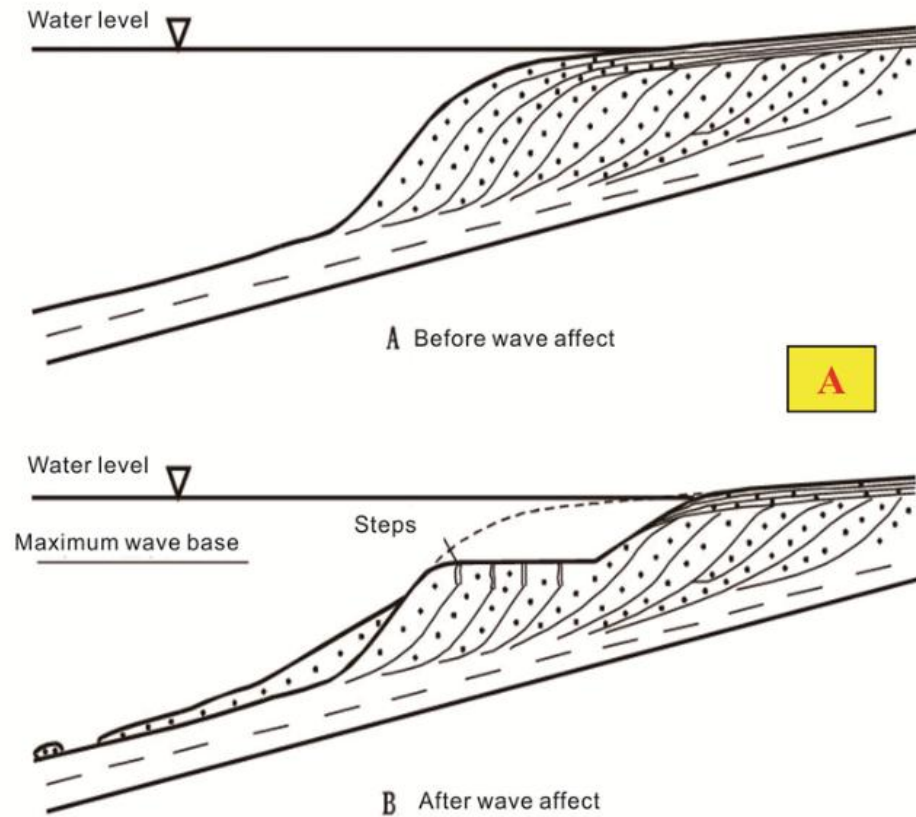


Figure 8. Flume experiments and the conceptual model of wave flapping mechanism. A: Turbidite formation manuscript. B: Sands are liquefied. C: Sand subsidence happens near maximum wave base.



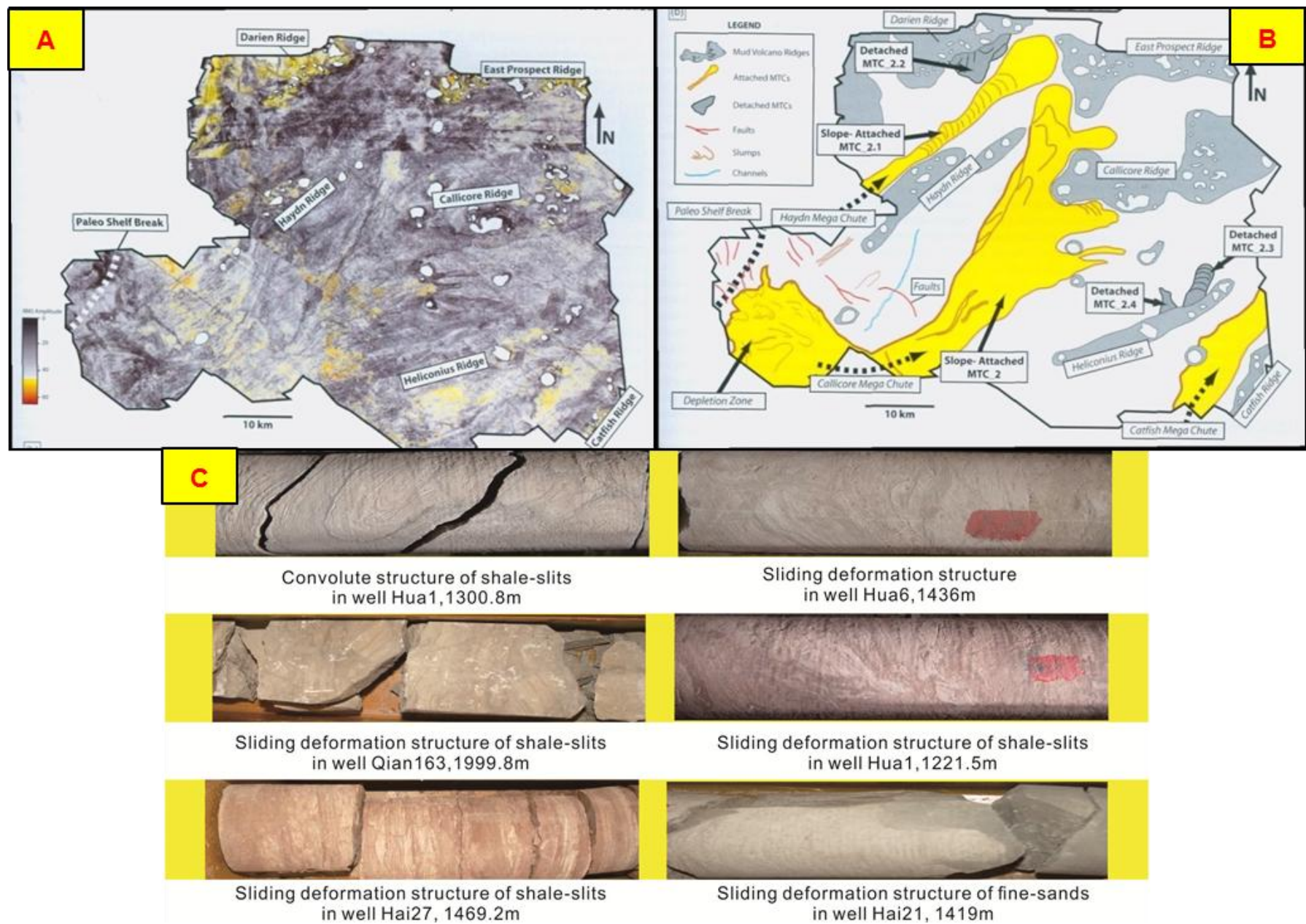


Figure 9. Turbidite slumps in Trinidad and Tobago of Pliocene-Pleistocene (Moscardelli and Wood, 2008), and core analysis in the Dabusu Area. A: RMS turbidite distribution. B: Interpreted turbidite slumps distribution. C: Different beddings in core analysis.



Complex analysis of sequence stratigraphy, sedimentary facies and cores in well Hua30

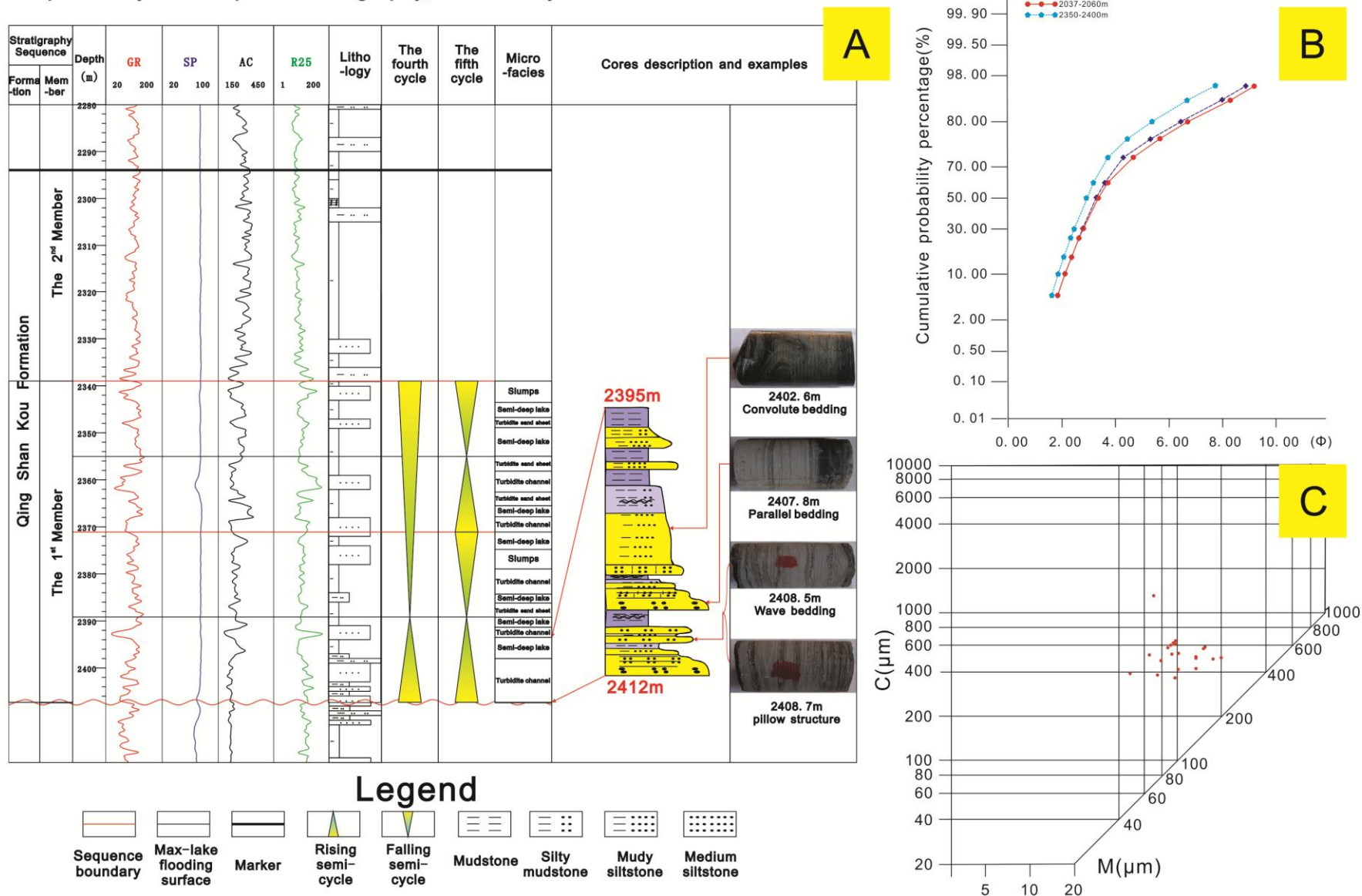


Figure 10. Sedimentary characteristics of cores in well Hua30. A: Comprehensive analysis of sedimentary facies analysis and core data observation. B: The cumulative probability percentage cartogram in different depth. C: The C-M cartogram in well Hua30.

## Sedimentary facies distribution of Q1 member in Dabusu area, SW Songliao basin

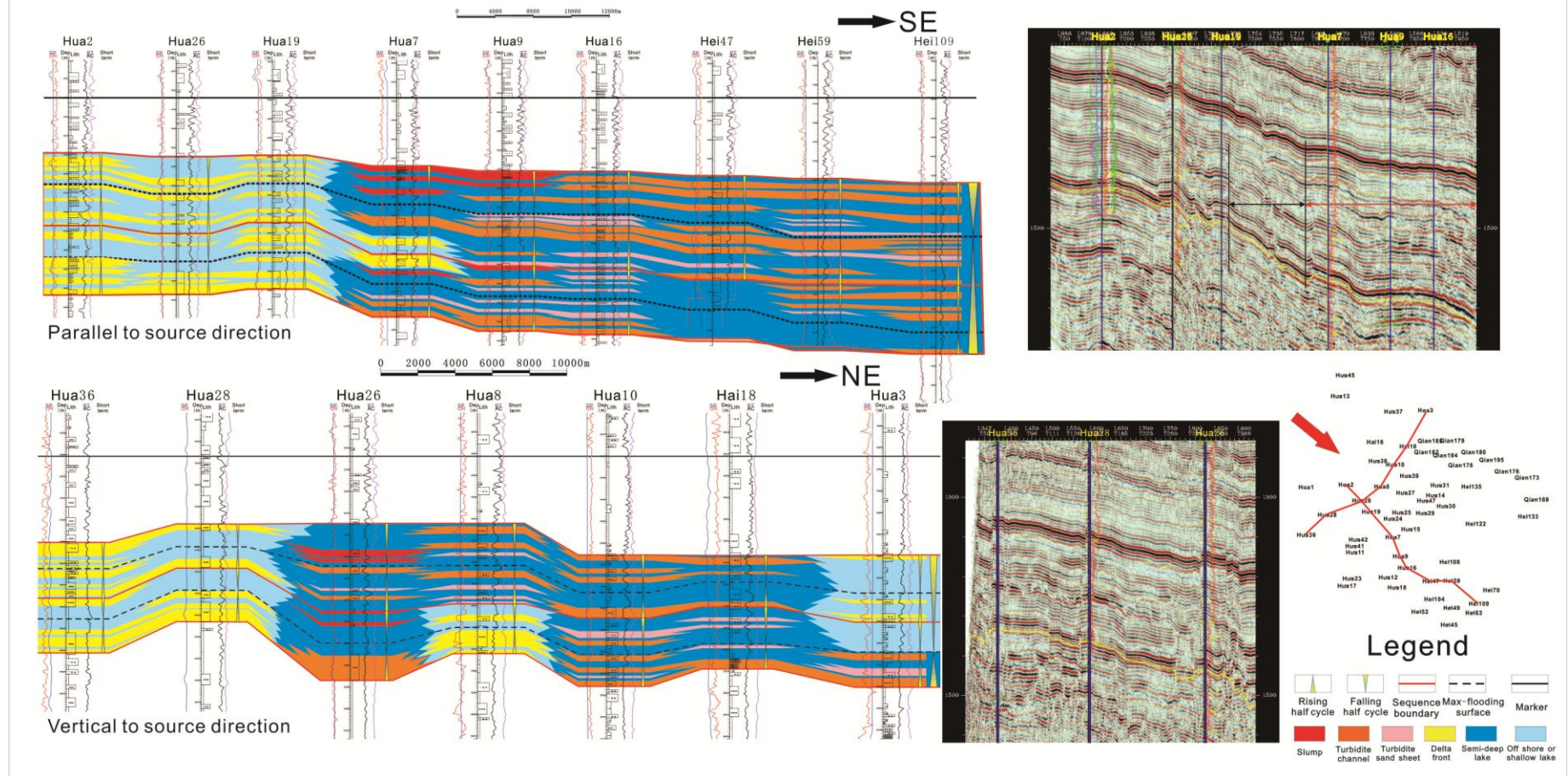


Figure 11. Different directions of sedimentary facies correlation. The upper Figure is parallel to the SSD, from a northwest to southeast direction. The lower Figure is vertical to the SSD, from a southwest to northeast direction.



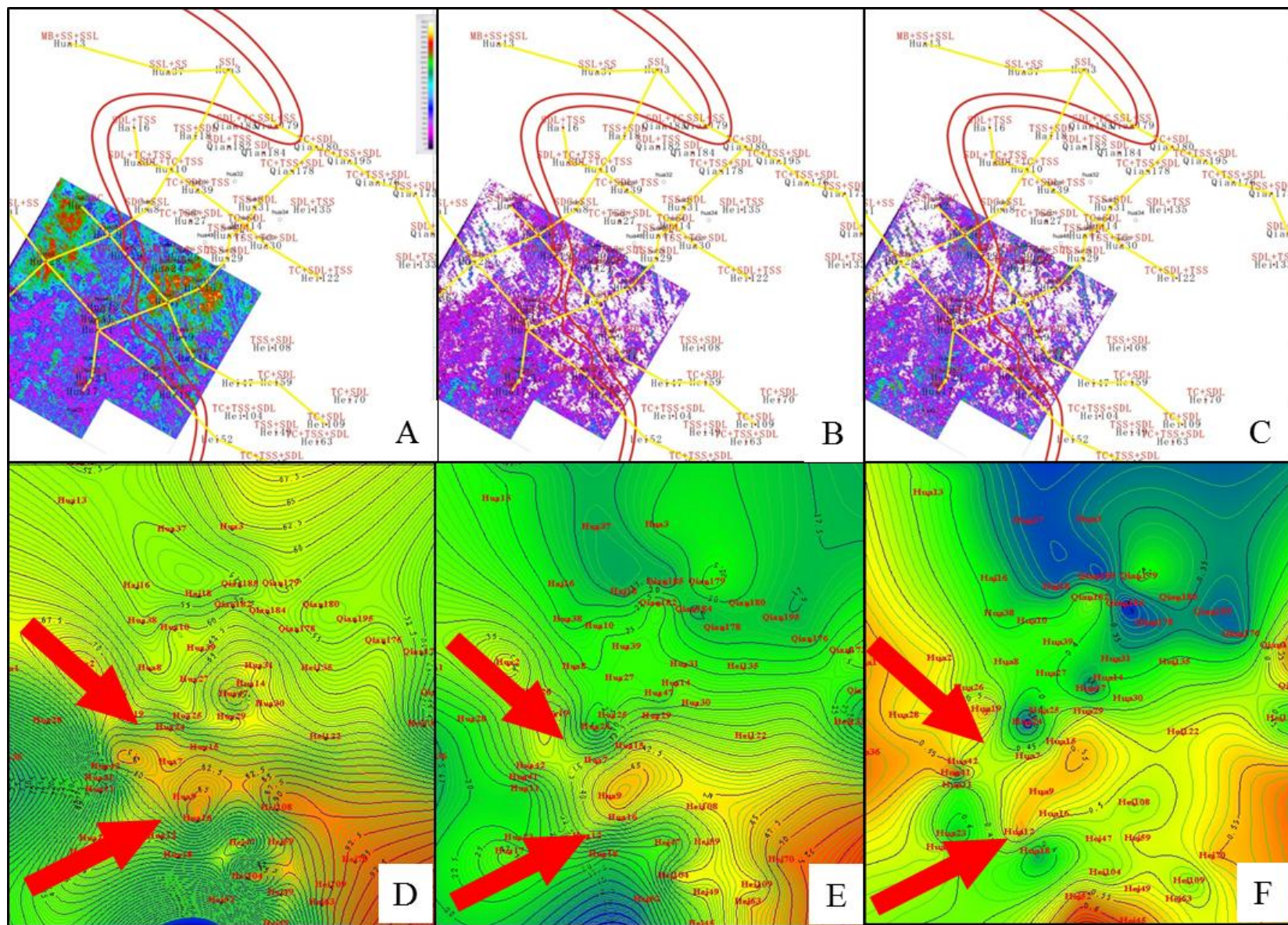


Figure 12. Seismic attributes and various thicknesses distribution in the falling period of the Kqn<sup>1</sup> Member in the west slope of the Dabusu Area, South Songliao Basin. Note: The area between the red lines is the slope, yellow lines are well section lines. A: RMS. B: The average wave amplitude. C: The maximum wave amplitude. D: The bed thickness. E: The sand thickness. F: The sand/bed ratio. The maximum dip angle is the optimal direction where source supplies go through, as shown by the red arrows.



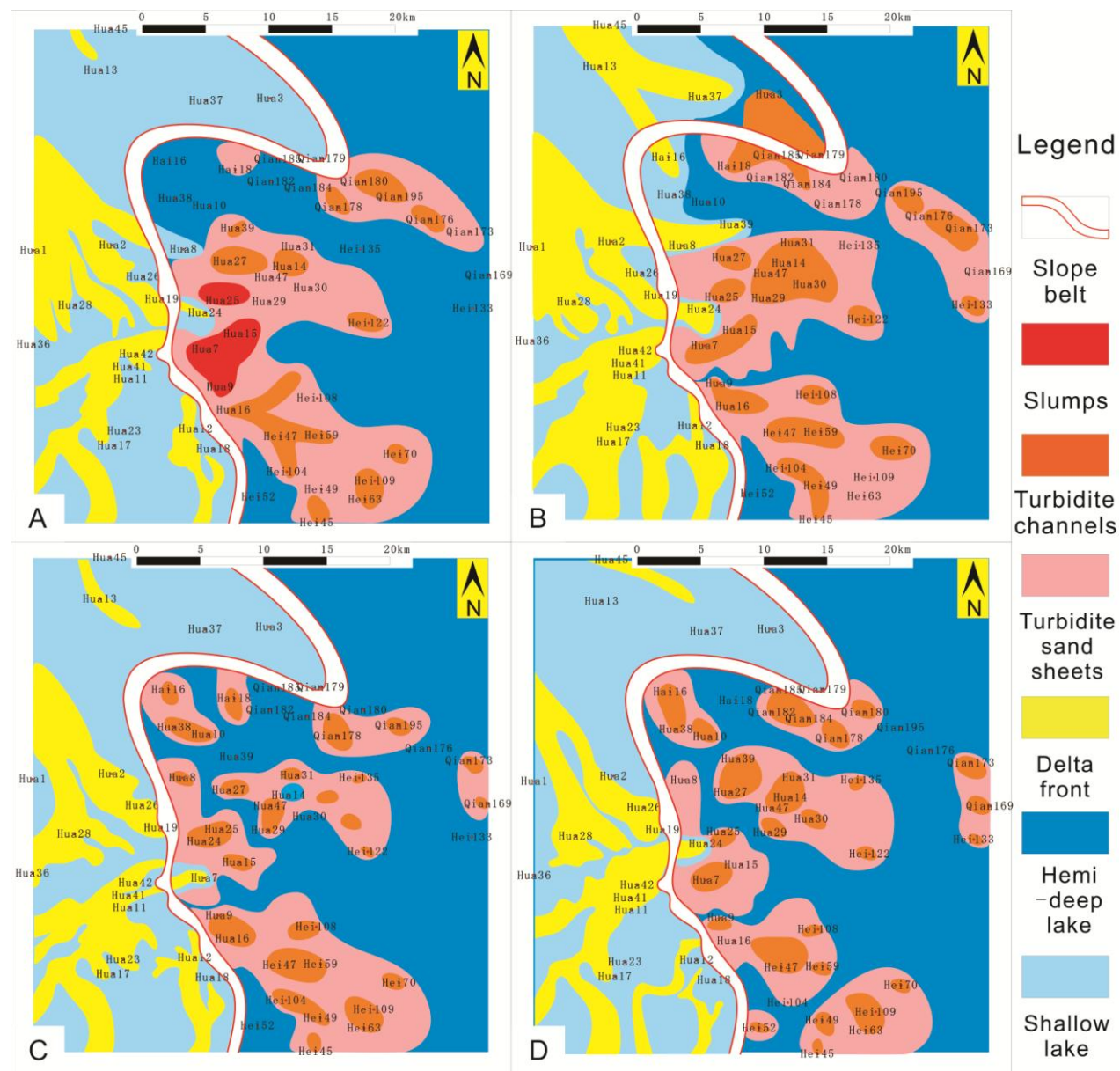


Figure 13. Sedimentary facies distribution of the Kqn<sup>1</sup> Member in the west slope of the Dabusu Area, South Songliao Basin. A: Sedimentary facies map in the falling period of Kqn<sup>1-1</sup> epoch. B: Sedimentary facies map in the rising period of the Kqn<sup>1-1</sup> epoch. C: Sedimentary facies map in the falling period of Kqn<sup>1-2</sup> epoch. D: Sedimentary facies map in the rising period of the Kqn<sup>1-2</sup> epoch.

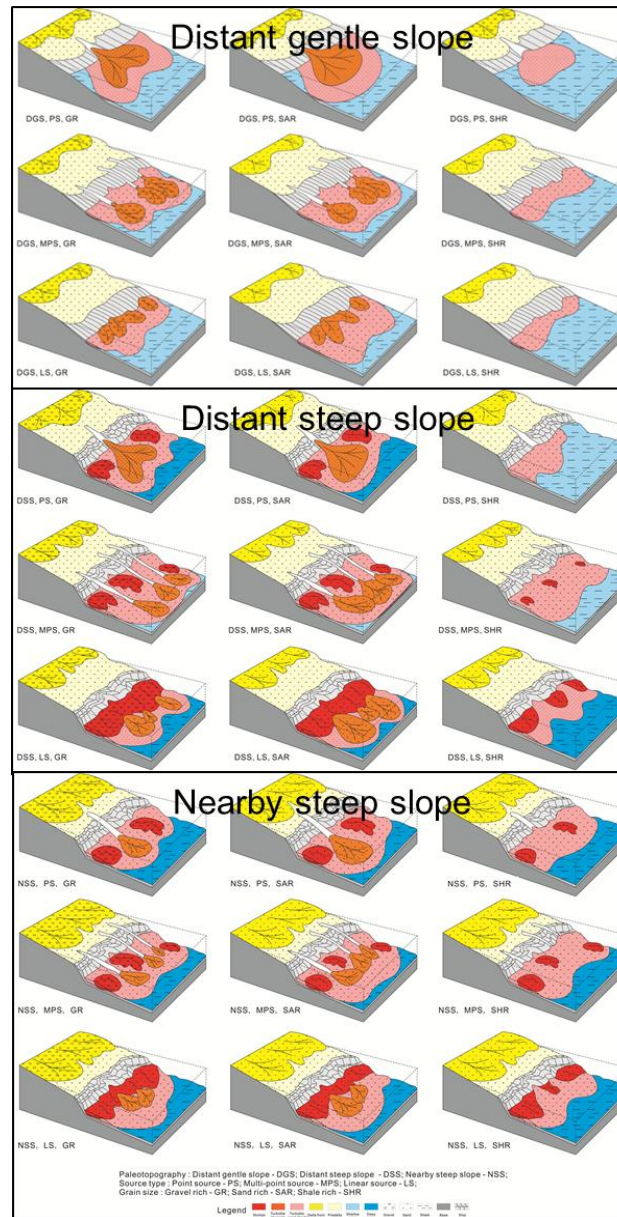


Figure 14. 27 types of turbidite depositional models. Three classes are: distant gentle slope, distant steep slope, and nearby steep slope. Source types are: point source, multi-point source, and linear source. According to grain size turbidities can be divided into: gravel rich, sand rich, and shale rich.

Oilfield name	Location	Year	Reservoir stratum	Recoverable reserves(BBL)
Wilmington	California	1932	Miocene-Pliocene	2.98
Fotis	North Sea	1970	Eocene	2
Maleme	Brazil	1985	Oligocene	1.83
Huntington	California	1920	Miocene-Pliocene	1.23
Friege	North Sea	1971	Paleocene	1.18

Table 1. Great oilfields produced from turbidities from all over the world (BBL=Billion barrel).



Kqn formation	BLC	Delta front deposits			Turbidite deposits				
		Distribution area (km <sup>2</sup> )	Thickness (m)	Well number	Distribution area (km <sup>2</sup> )			Thickness (m)	Well number
					Slumps	Turbidite channels	Turbidite sand sheets		
Kqn <sup>1-1</sup>	Falling	1.60	5.06	20	0.25	0.62	3.19	6.17	38
	Rising	2.62	9.39	21	0.00	1.23	3.48	8.22	37
Kqn <sup>1-2</sup>	Falling	1.66	5.58	19	0.00	0.70	3.01	7.41	39
	Rising	1.47	6.60	19	0.00	0.84	3.11	8.30	39

Table 2. Statistics of delta front sands and turbidite sands distribution.